

# Fracture Fabrication of a Multi-scale, Channel Device that Efficiently Captures and Linearizes DNA from Dilute Solutions

Byoung Choul Kim<sup>1,2,3</sup>, Priyan Weerappuli<sup>1,3</sup>, M.D. Thouless<sup>4,5</sup>, and Shuichi Takayama<sup>1,2,3,6</sup>

<sup>1</sup>*Department of Biomedical Engineering, College of Engineering, University of Michigan, 2200 Bonisteel Blvd, Ann Arbor, MI 48109, USA*

<sup>2</sup>*Macromolecular Science and Engineering Center, College of Engineering, University of Michigan, 2300 Hayward St., Ann Arbor, MI 48109, USA*

<sup>3</sup>*Biointerfaces institute, University of Michigan, 2800 Plymouth Rd, Ann Arbor, MI 48109, USA*

<sup>4</sup>*Department of Mechanical Engineering, College of Engineering, University of Michigan, 2350 Hayward St., Ann Arbor, MI 48109, USA*

<sup>5</sup>*Department of Materials Science & Engineering, College of Engineering, University of Michigan, 2300 Hayward St., Ann Arbor, MI 48109, USA*

<sup>6</sup>*Division of Nano-Bio and Chemical Engineering WCU Project, UNIST, Ulsan, Republic of Korea*

\* e-mail: [takayama@umich.edu](mailto:takayama@umich.edu)

## Abstract

This paper describes a simple technique for patterning channels on elastomeric substrates, at two distinct scales of depth, through the use of controlled fracture. Control of channel depth is achieved by the careful use of different layers of PDMS, where the thickness and material properties of each layer, and the position of layers relative to one another, dictate the depth of the channels formed. The system created in this work consists of a single ‘deep’ channel, whose width can be adjusted between the micron- and nano-scale by the controlled application or removal of a uniaxial strain, and an array of ‘shallow’ nano-scale channels oriented perpendicular to the ‘deep’ channel. The utility of this system is demonstrated through the successful capture and linearization of DNA from a dilute solution, by executing a two-step ‘concentrate-then-linearize’ procedure. When the ‘deep’ channel is in its open state, and a voltage is applied across the channel network, an overlapping electric double layer forms within the ‘shallow’ channel array. This overlapping electric double layer is used to prevent passage of DNA into the ‘shallow’ channels when the DNA molecules migrate into the junctional region by electrophoresis. Release of the applied strain then allows the ‘deep’ channel to return to its closed state, reducing the cross-sectional area of this channel from the micron- to the nano-scale. The resulting hydrodynamic flow and nano-confinement effects then combine to efficiently uncoil and trap the DNA in its linearized form. By adopting this strategy, we were able to overcome the entropic barriers associated with capturing and linearizing DNA derived from a dilute solution.

## Introduction

Fabrication techniques capable of producing features at both the micro- and nano-scales, present novel opportunities for pursuing broad biological applications; including more efficient sample preparation, pre-processing, and analysis at both the cellular and molecular level.<sup>1-7</sup> The fabrication of multi-scale features by conventional methods requires complex procedures, careful handling, and the use of specific materials and expensive equipment. Consequently, it is generally a much more difficult task than the fabrication of mono-scale features. In previous work, we have reported the use of controlled-fracture to fabricate channels at the micro- and nano-scales by the use of multi-layered structures, where channel depth is controlled by the properties and dimensions of the individual layers. Furthermore, we have also reported the capacity to produce uniform arrays of size-adjustable channels by judicious positioning of stress-shielding structures.<sup>8</sup> Here, we combine these various procedures to develop a simple approach for creating multi-scale patterns using controlled fracture.

We report a technique which we have used successfully to produce orthogonally-oriented channels of differing scales using multi-layered assemblies comprised of poly(dimethylsiloxane) (PDMS) and its variant, hard-PDMS (h-PDMS). The resulting channel system consisted of a ‘deep’ single channel, whose cross-sectional area could be stably adjusted between the micron- and nano-scale by the application of sustained uniaxial strain; intersected by a ‘shallow’, fixed-width, nano-scale channel array. This unique system was used to conduct a nano-confinement-based single-DNA analysis, where the DNA studied was derived from a dilute solution.

The introduction of DNA into nanochannels has traditionally been most efficient when the initial sample concentration is high, or when an external force is applied.<sup>9-11</sup> This is the result of two fundamental challenges associated with capturing DNA from dilute solutions within a nanochannel geometry: the entropic cost of concentrating DNA molecules within a small volume, and the entropic cost associated with uncoiling DNA.<sup>11, 12</sup> In this paper, our channel system was employed to overcome such challenges by sequentially exploiting (i) nanochannel-based electrophoretic movement to position single DNA molecules in a desired location, and (ii) tunable modulation of channel width to induce uncoiling of the DNA.

## Materials and Methods

### Criss-crossing ‘deep’/‘shallow’ channel fabrication

A carefully-planned sequence of material layering and strain application is used to create a four-layered structure with criss-crossing ‘deep’/‘shallow’ channels. The four-layers making up this structure are (i) PDMS (capping layer), (ii) silica-like h-PDMS (SL-h-PDMS), (iii) hPDMS, and (iv) PDMS (substrate layer). The thickness and modulus differences between these four layers determine which layer cracks are formed in, and the size of the resulting cracks. Strategically placed features molded into the structures using conventional micro-fabrication methods,<sup>13</sup> serve the dual roles of controlling crack location and functioning as liquid reservoirs during operation of the device.

Opposing pairs of micron-scale, sharp, V-notch reservoirs and blunt reservoirs were cast into an h-PDMS elastomer mixture as previously described,<sup>14</sup> and spin-coated directly on a master-mold consisting of SU-8 (Microchem) features patterned upon a polished silicon wafer. The sharp and blunt reservoirs were aligned perpendicular to one another. This h-PDMS layer (target thickness: ~ 10 microns) was then incubated at 120°C for 120 s. Following incubation, a 10:1 mixture of PDMS monomer and a Sylgard 184 cross-linker (Dow Corning) was deposited above the h-PDMS layer to a target thickness of 5 mm, and cured overnight at 60°C. The cured h-PDMS/PDMS bilayer was then carefully peeled from the SU-8 mold, and loaded into a stretcher (S.T. Japan USA LLC, FL, USA). When a uniaxial strain of approximately 15% was applied in a direction perpendicular to the V-notch tips, a single crack was initiated at each tip. These propagated uni-directionally until a complete crack was formed between the tips. A thorough characterization of such crack formation, and its control, is presented in earlier work.<sup>8,15</sup> This ‘deep’ crack occurred at the micron-scale, corresponding to the thickness of the h-PDMS layer. The applied strain was then removed, and the h-PDMS layer was covered with tape (3M, Inc.), so that only the region between the blunt reservoirs remained exposed. This region was then selectively treated by plasma oxidation (200W, 600s), to create a thin silica-like surface (SL-h-PDMS). After removing the tape, a uniaxial strain of approximately 6% was applied in a direction perpendicular to the blunt-tip features to induce the formation of multiple ‘shallow’ cracks between the blunt micro-features that were positioned orthogonal to the original deep crack. This second set of the ‘shallow’ cracks occurred at the nano-scale, corresponding to the thickness of the SL-h-PDMS layer. The resulting SL-h-PDMS/h-PDMS/PDMS tri-layer was then bonded to a PDMS membrane (target thickness: 200 μm) to convert these fractures, through sealing, into the single ‘deep’/multiple ‘shallow’ channel pattern.

### **Electrophoretic DNA migration and stacking at ‘deep’/‘shallow’ channel interface**

All reservoirs and channels were perfused with 0.1x TBE buffer. Following perfusion, a λ-DNA solution (100 pg/μl, New England Biolabs, Inc), stained with YOYO-1 intercalating dye at a base-pair to dye ratio of 20:1, was loaded into the one of the sharp-tip reservoirs. A cathode was then positioned in the same sharp-tip reservoir, and a corresponding anode was positioned in one of the blunt tip reservoirs. The coincident application of uniaxial strain along the axis perpendicular to the ‘deep’ channel, and an electric field (80V), was used to induce DNA pre-concentration at the juncture between the ‘shallow’ and ‘deep’ channels, the latter now in its open state. Electrophoretic DNA stacking was recorded with a 20x objective installed in a Nikon Ti-U microscope.

### **Single DNA capture and elongation in hybrid micro-nanochannel structure**

A low concentration λ-DNA solution (1 pg/μl) was loaded into the four-layer assembly; after which a cathode and anode were positioned within the device, as previously described. A mild electric field (40V) was then applied while the ‘deep’ channel was held in its open state by the sustained application of uniaxial strain. The presence of this electric field caused the λ-DNA molecule in the solution to migrate through the open ‘deep’ channel toward the intersecting ‘shallow’ channels. The inability of the DNA to enter the ‘shallow’ channels, however, resulted in single molecules being stranded at this junction. The stranded λ-DNA molecule was then linearized by the controlled release of the applied strain, which induced narrowing of the ‘deep’ channel to its closed state.

## Results & Discussion

### Size-controllable channel structures for concentration, trapping, and elongation of DNA

As described above, the device used in these experiments consisted of a single ‘deep’ channel connecting the two sharp-tip reservoirs, and an array of ‘shallow’ channels connecting the blunt-tip reservoirs (Figure 1a). Application of uniaxial strain in the direction perpendicular to the axis delineated by the sharp-tip reservoirs opened the normally-closed ‘deep’ channel (Figure 1b). Subsequent application of an electric field across the channel network then induced electrophoretic movement of DNA molecules to the junction between the ‘shallow’ channels and the open ‘deep’ channel (Figure 1c). After successfully positioning the molecule at this junction, the applied strain was released, to generate hydrodynamic forces that elongated and linearized the DNA as the ‘deep’ channel passively returned to its closed state (Figure 1d).

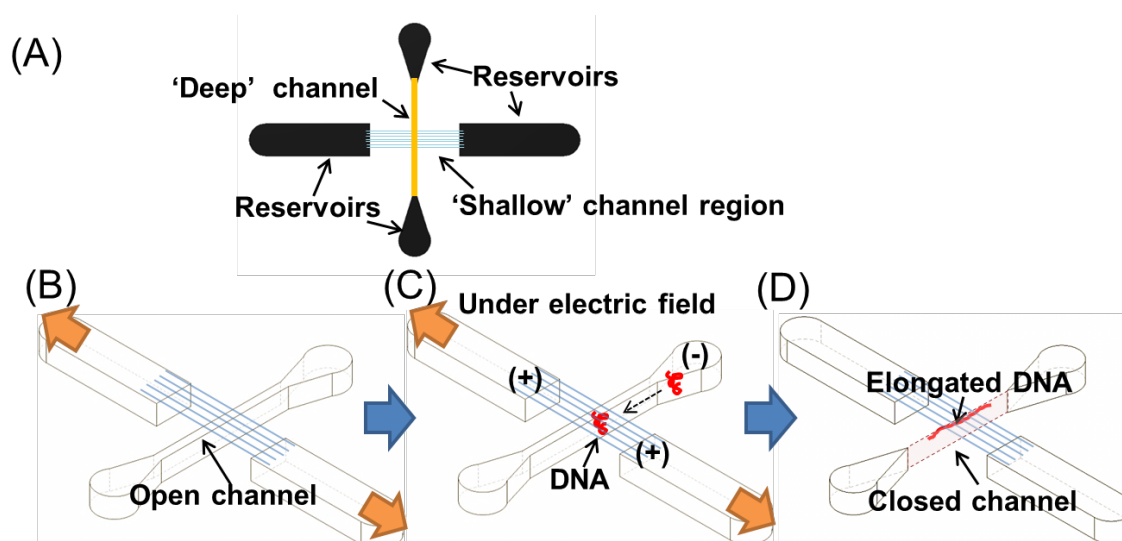


Figure 1. Schematic of DNA migration and squeezing system. (A) A single ‘deep’ channel and multiple perpendicularly-oriented ‘shallow’ channels. Each fracture-formed structure originates, and terminates, within a reservoir so that ‘shallow’ channels effectively connect the blunt-tip reservoirs, while the ‘deep’ channel connects the sharp-tip reservoirs. In its operation, (B) the ‘deep’ channel is transitioned from a closed to an open-state through the application of a uniaxial strain along an axis perpendicular to the ‘deep’ channel itself. When in its open state, (C) DNA introduced via one of the sharp-tip reservoirs will migrate and become localized at the juncture between the ‘deep’ channel and its intersecting ‘shallow’ channels through exclusion-enrichment effect. (D) The subsequent release of the previously-applied uniaxial strain then allows the ‘deep’ channel to return to its closed-state, and in doing so, generates hydrodynamic flow within the channel sufficient to linearize the trapped DNA molecule.

### **Fracture fabrication procedures to create the criss-crossing ‘deep’/‘shallow’ channel device**

The different fracture characteristics of h-PDMS and SL-h-PDMS<sup>2, 9, 11-14</sup> were used to generate intersecting cracks of differing scale. Summarizing previous work, the fracturing of films produced by the plasma oxidation of PDMS (referred to as silica-like PDMS (SL-PDMS)) result in the formation of nano-scale channels, owing to the thin and brittle nature of the SL-PDMS layer<sup>2, 16, 17</sup>. Fracturing of h-PDMS deposited on a PDMS slab results in the formation of micron-scale channels, owing to the relatively thick and compliant nature of the h-PDMS film<sup>14</sup>. To construct the criss-crossing multi-scale ‘deep’/‘shallow’ channel device presented herein; we first formed a single, normally-closed ‘deep’ channel within an h-PDMS/PDMS bilayer structure using pre-patterned stress-shielding features and controlled fracture<sup>8, 14, 15</sup>. Next, we speculated, and confirmed, that plasma treatment of h-PDMS creates a thin SL-h-PDMS layer that forms nano-scale cracks. By restricting the region of the h-PDMS surface exposed to plasma oxidation through judicious use of a tape mask (Figure 2D), and by applying the cracking strain in a direction perpendicular to the direction used for formation of the ‘deep’ channel, an array of ‘shallow’ nano-scale channels was formed perpendicular to the original ‘normally-closed’ ‘deep’ channel. This ensured that any fluid communication between the ‘deep’ and ‘shallow’ channels occurred only at their points of intersection (Figure 2, and see Materials and Method section). In the resulting device, the multiple ‘shallow’ channels formed in the SL-h-PDMS layer remained slightly open at the nano-scale, even in the absence of an applied strain, owing to residual stresses resulting from the plasma oxidation<sup>18, 19</sup>.

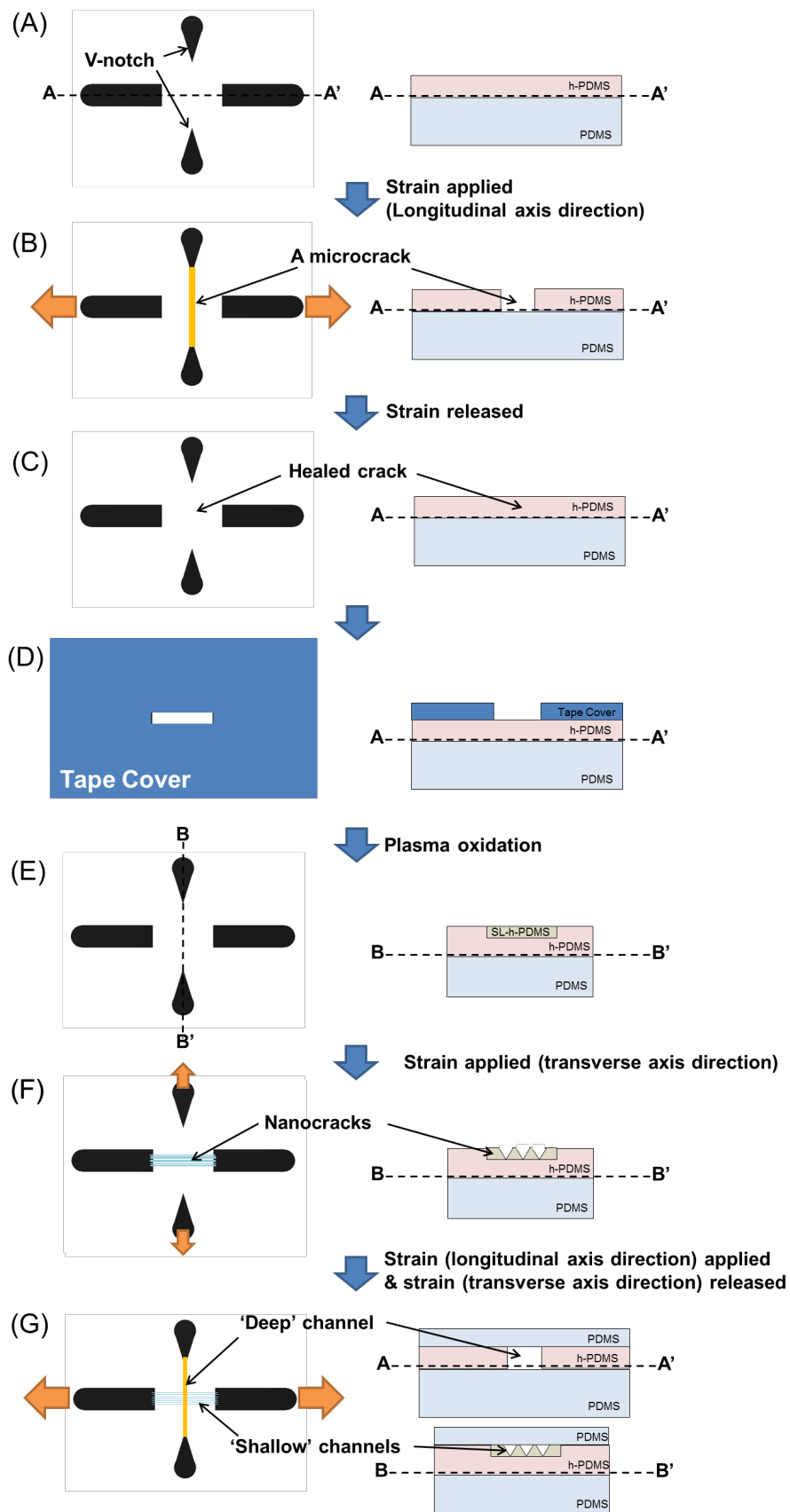


Figure 2. A diagram of the stepwise fabrication process used for the fabrication of the described criss-crossing channel system. (A) Two pairs of symmetrical micro-features were first cast within the h-PDMS/PDMS bilayer assembly from a pre-patterned SU-8 mold. (B) A single crack was then formed in the h-PDMS layer. This crack extended between the mirrored V-notch tips by the controlled application of uniaxial strain, and was capable of being (C) ‘healed’ (closed and bonded through van der Waals forces) upon release of the applied strain. (D) The two-layer assembly was then covered by a tape mask so that only the surface region between the blunt-tip features was exposed. This enabled the (E) selective plasma-treatment of this region, producing a SL-h-PDMS nano-layer on the surface of the h-PDMS layer. (F) Multiple nano-cracks were then produced in the SL-h-PDMS layer when the assembly was subjected to a second uniaxial strain applied in a direction perpendicular to that of the previously applied strain. The resulting cracks were then sealed by plasma bonding the cracked-surface to a PDMS membrane, forming (G) a single ‘deep’ channel in the h-PDMS layer and multiple orthogonally-oriented ‘shallow’ channels in the SL-h-PDMS.

### **Electrophoretic DNA migration by ion concentration polarization (ICP)**

The functional significance of the ‘shallow’ channel array within this system, is its capacity to facilitate pre-concentration of negatively charged DNA molecules by providing a structural environment capable of generating an exclusion-enrichment effect (EEE) induced by ion-concentration polarization (ICP).<sup>20-22</sup> Here, the narrow width of the nano-scale ‘shallow’ channels produces overlapping electrical double layers (EDLs) within each channel that restrict the directionality of ion transfer upon application of an external electric potential.<sup>20, 23, 24</sup> Consequently, the negative surface charge on the SL-h-PDMS layer, combined with the presence of EDLs within the ‘shallow’ channels, prevent  $\lambda$ -DNA molecules from being able to enter these channels after they have been drawn along the ‘deep’ channel (in its open state) from the cathodic sharp-tip reservoir (Figure 3A). By extension, the presence of these channels, under a stronger electric field, or through more prolonged exposure to a relatively mild external electric field, may also facilitate DNA stacking, as multiple DNA molecules are allowed to migrate through the ‘deep’ channel and aggregate at the junction between the ‘deep’ and ‘shallow’ channels (Supplementary Figure 1).

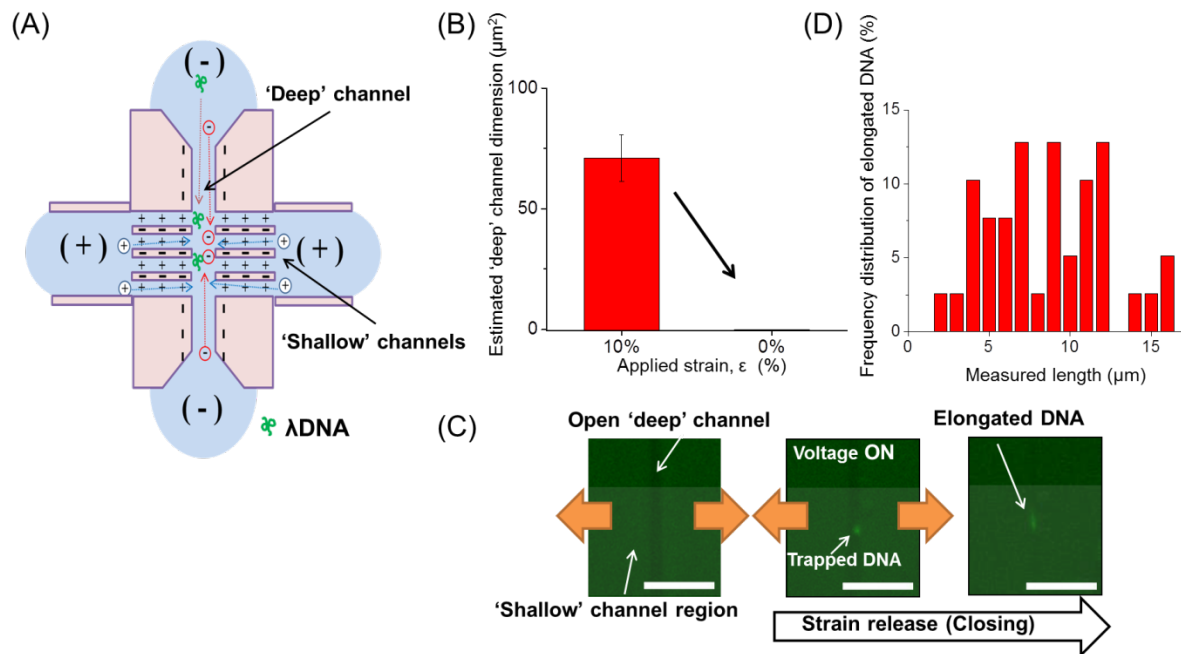


Figure 3. Application of the ‘deep’/‘shallow’ channel system for capturing and elongating single DNA molecules. (A) A schematic illustrating the ion concentration polarization and DNA migration generated within the ‘deep’/‘shallow’ channel junction under an applied electric field. (B) Changes in the cross-sectional dimensions of the ‘deep’ channel in response to a sustained applied strain. (C) An illustration of the multiple steps involved in DNA concentration, trapping, and linearization in the ‘deep’ channel. The gray color represents the ‘shallow’ nano-scale channel region. Scale bar is 100  $\mu\text{m}$ . (D) A plot of the frequency distribution of the lengths of elongated  $\lambda$ -DNA in the closed ‘deep’ channel.

### Single DNA capturing and linearization in the ‘deep’ channel

Based on the theoretical background of electrophoretic DNA migration in the criss-crossing channel device, we conducted single DNA capturing and linearization using a very low concentration  $\lambda$ -DNA solution (1 pg/ $\mu\text{l}$ ). Following sample loading, the ‘deep’ channel, extending between the sharp-tip reservoirs, was opened, and a mild electric field (approximately 40V) was applied to localize a single DNA molecule at the ‘deep’/‘shallow’ channel junction. The ‘deep’ channel could be expanded to a cross-sectional area of approximately 70  $\mu\text{m}^2$  in its open state (under 10% strain), and reduced to approximately 1220  $\text{nm}^2$  in the absence of an applied strain (Figure 3B). This cross-sectional size-adjustability of the ‘deep’ channel enabled easy loading of  $\lambda$ -DNA into the strain-widened channel under an applied electric field and, also, circumvented the entropic costs associated with  $\lambda$ -DNA uncoiling, by coupling this process with the reduction in channel width initiated by the release of the previously-applied strain. By doing so, DNA linearization was performed passively by simply exploiting the hydrodynamic forces and nanoconfinement effects produced during the narrowing of the ‘deep’ channel to its normally-closed nano-scale dimensions (Figure 3C). The calculated DNA concentration achieved following channel narrowing was approximately 145 ng/ $\mu\text{l}$ , which is nearly 145,000x higher relative to the concentration of the initial stock solution. The calculated degree of linearization of the trapped DNA ( $n = 39$ ) in the closed ‘deep’ channel was  $52 \pm 20\%$  relative to the



contour length of  $\lambda$ -DNA considering intercalating dye effects (expected full length of  $\lambda$ -DNA under the dye concentration used is approximately 17.5  $\mu$ ). These results suggest that the entropic challenge to un-coiling DNA is also overcome despite slight deficits in the extent of linearization observed, owing to DNA adsorption to the channel wall, or partial channel collapse (Figure 3D).

## Conclusions

We have developed a simple method to fabricate criss-crossing ‘deep’/‘shallow’ channels in multi-layered soft materials by a fracture-based technique. Careful control of the thickness and properties of each layer provided the capacity to pattern differentially-sized fractures. Stress-shielding features and applied strain (both magnitude and direction) were then used to generate a hybrid micro/nanochannel system. To our knowledge, this is the first reported approach to develop multi-scaled channel structures in such a robust, yet simple, manner. This paper expands the capabilities of fracture-based micro/nanofabrication. Importantly, this fabrication technique was applied to create a unique and useful fluidic platform capable, in itself, of overcoming inherent entropic barriers to efficiently pre-concentrate and linearize single DNA molecules isolated from a sample with low initial concentration. These barriers, the entropic costs of concentrating and uncoiling DNA, are overcome by exploiting the exclusion-enrichment effect and ion-concentration polarization, to produce efficient electrophoretic pre-concentration. The use of hydrodynamic shear, generated by the controlled release of an applied strain, then uncoiled these DNA molecules within the size-adjustable channels. In addition to the successful manipulation of DNA that has been reported here, criss-crossing arrangements of channels have demonstrated their utility in a variety of applications including the handling of worms<sup>25, 26</sup> or bacteria,<sup>27</sup> oocyte cryopreservation<sup>28</sup>, and single cell analysis.<sup>29</sup> Owing to the versatility of the fracture-based fabrication method for the fabrication of channels in producing differing micro- and nano-scale channels, we believe this fabrication method and device will prove to have broader applications beyond the specific example presented here.

## Acknowledgments

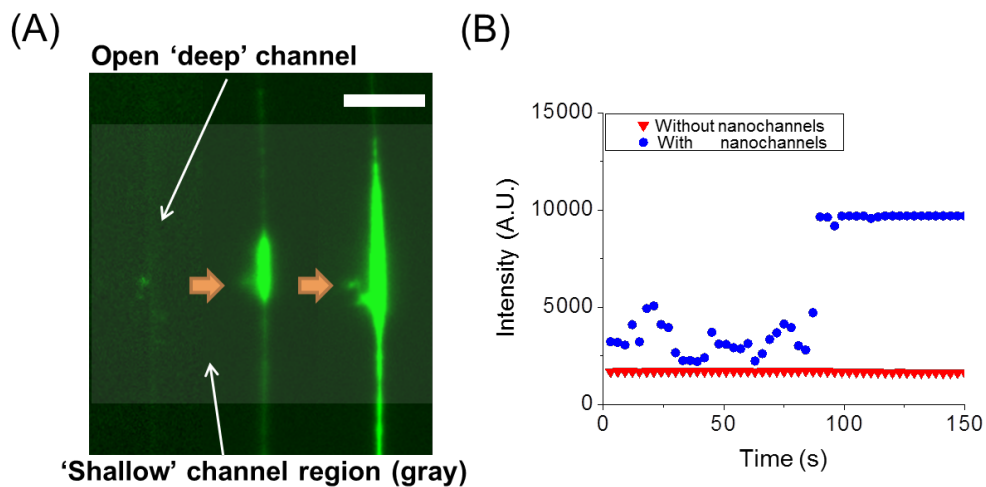
This work was supported by a grant from the US National Institute of Health (HG004653-03), a Rare Cells Seed Grant from the Biointerfaces Institute, University of Michigan (to BCK), and the Wayne State University Interdisciplinary Biomedical Sciences Competitive Research Fellowship (to PW).

## References

1. S. F. L. Diana E. Streng, Junhan Pan, Alena Karpusenka and Robert Riehn *Lab on a Chip*, 2009, **9**, 2772-2774.
2. T. Matsuoka, B. C. Kim, J. Huang, N. J. Douville, M. Thouless and S. Takayama, *Nano letters*, 2012.
3. T. Matsuoka, B. C. Kim, C. Moraes, M. Han and S. Takayama, *Biomicrofluidics*, 2013, **7**, 041301.
4. C. A. Aguilar and H. G. Craighead, *Nature Nanotechnology*, 2013, **8**, 709-718.

5. H. Cao, J. O. Tegenfeldt, R. H. Austin and S. Y. Chou, *Applied Physics Letters*, 2002, **81**, 3058-3060.
6. F. Persson and J. O. Tegenfeldt, *Chemical Society Reviews*, 2010, **39**, 985-999.
7. E. T. Lam, A. Hastie, C. Lin, D. Ehrlich, S. K. Das, M. D. Austin, P. Deshpande, H. Cao, N. Nagarajan and M. Xiao, *Nat Biotechnol*, 2012, **30**, 771-776.
8. B. C. Kim, T. Matsuoka, C. Moraes, J. Huang, M. Thouless and S. Takayama, *Scientific reports*, 2013, **3**.
9. W. Reisner, J. N. Pedersen and R. H. Austin, *Reports on Progress in Physics*, 2012, **75**, 106601.
10. J. Han and H. Craighead, *Science*, 2000, **288**, 1026-1029.
11. M. Cabodi, S. W. Turner and H. G. Craighead, *Analytical chemistry*, 2002, **74**, 5169-5174.
12. J. Mannion, C. Reccius, J. Cross and H. Craighead, *Biophysical journal*, 2006, **90**, 4538-4545.
13. Y. Xia and G. M. Whitesides, *Annual review of materials science*, 1998, **28**, 153-184.
14. B. C. Kim, C. Moraes, J. Huang, T. Matsuoka, M. Thouless and S. Takayama, *Small*, 2014.
15. J. Huang, B. C. Kim, S. Takayama and M. Thouless, *Journal of Materials Science*, 2014, **49**, 255-268.
16. K. L. Mills, D. Huh, S. Takayama and M. D. Thouless, *Lab Chip*, 2010, **10**, 1627-1630.
17. D. Huh, K. Mills, X. Zhu, M. A. Burns, M. Thouless and S. Takayama, *Nature materials*, 2007, **6**, 424-428.
18. M. D. Thouless, Z. Li, N. Douville and S. Takayama, *Journal of the Mechanics and Physics of Solids*, 2011.
19. N. J. Douville, Z. Li, S. Takayama and M. D. Thouless, *Soft Matter*, 2011, **7**, 6493-6500.
20. S. J. Kim, Y.-A. Song and J. Han, *Chemical Society Reviews*, 2010, **39**, 912-922.
21. H. Kim, J. Kim, E.-G. Kim, A. J. Heinz, S. Kwon and H. Chun, *Biomicrofluidics*, 2010, **4**, 043014.
22. Z.-Y. Wu, C.-Y. Li, X.-L. Guo, B. Li, D.-W. Zhang, Y. Xu and F. Fang, *Lab Chip*, 2012, **12**, 3408-3412.
23. R. Chantiwas, S. Park, S. A. Soper, B. C. Kim, S. Takayama, V. Sunkara, H. Hwang and Y.-K. Cho, *Chemical Society Reviews*, 2011, **40**, 3677-3702.
24. W. Sparreboom, A. Van Den Berg and J. Eijkel, *Nature Nanotechnology*, 2009, **4**, 713-720.
25. N. Chronis, M. Zimmer and C. I. Bargmann, *Nature methods*, 2007, **4**, 727-731.
26. C. B. Rohde, F. Zeng, R. Gonzalez-Rubio, M. Angel and M. F. Yanik, *Proceedings of the National Academy of Sciences*, 2007, **104**, 13891-13895.
27. N. Tandogan, P. N. Abadian, S. Epstein, Y. Aoi and E. D. Goluch, *PloS one*, 2014, **9**, e101429.
28. D. J. Lai D., Smith G.W., Smith G.D., Takayama S., *Hum Reprod*, 2014, **Accepted**.
29. D. Di Carlo, N. Aghdam and L. P. Lee, *Analytical chemistry*, 2006, **78**, 4925-4930.

## Supporting Information



Supplementary Figure 1. Electrophoretic stacking of DNA at the 'deep'/'shallow' criss-crossing channel interface under exposure to a strong, prolonged electric field. (A) Time-lapse images of DNA stacking at the entrance of the 'shallow' nano-scale channel region. Scale bar is 100  $\mu\text{m}$ . (B) Measured intensity of DNA with the existence of the 'shallow' channel region.

Time-lapse images (Figure 1A) were gathered to illustrate this process, and measure the local accumulation of  $\lambda$ -DNA at the 'deep'/'shallow' channel junction. This process was characterized, quantitatively, by the measured intensity of the stained DNA. Following one minute of applied voltage, the intensity of fluorescently-stained  $\lambda$ -DNA dramatically increased within the device, to the extent that the fluorescence-intensity became saturated within the field of view.